Three-Dimensional (3D) Modelling and Optimization for Multipurpose Analysis and Representation of Ancient Statues

(Article begins on next page)

26 April 2024

Three-Dimensional (3D) Modelling and Optimization for Multipurpose Analysis and Representation of Ancient Statues

Elisabetta Donadio [a]**, Luigi Sambuelli** [b]**, Antonia Spanò** [a] **and Daniela Picchi** [c]

[a] DAD Department, Politecnico di Torino, Italy; (elisabetta.donadio antonia.spano)@polito.it

[b] DIATI Department, Politecnico di Torino, Italy; luigi.sambuelli@polito.it

[c] Civic Archaeological Museum, Via dell'Archiginnasio 2, 40124 Bologna (Italy); daniela.picchi@comune.bologna.it

Abstract: The technological advances that have developed in the field of three-dimensional (3D) survey and modelling allow us to digitally and accurately preserve many significant heritage assets that are at risk. With regard to museum assets, extensive digitalization projects aim at achieving multilingual digital libraries accessible to everyone. A first trend is geared to the use of 3D models for further specialized studies, acquiring and processing virtual detailed copies as close as possible to the shape and contents of the real one. On the other hand, many museums look today for more interactive and immersive exhibitions, which involve the visitors' emotions, and this has contributed to the increase in the use of virtual reality and 3D models in museums installations. In this paper, we present two case studies that belong to these scenarios. Multisensor surveys have been applied to some archeological statues preserved in two museums for multipurpose analyses and representation: a UTI test, which required high detailed data about the geometry of the object, and a communicative application, which needed instead a high level of model optimization, poor geometry, but very good representation that was achieved through remeshing tools and normal maps.

Keywords: 3D models; normal map; remeshing; 3D Ultrasonic Tomographic Imaging (3D UTI); cultural heritage

1. Introduction

Many significant heritage assets around the world face different and continuous challenges due to the need of continuously evaluate the state of

conservation for future generations, or, even more for sites than for museum assets, due to the severe natural and hand-made hazards.

The technological advances that have developed in the field of three-dimensional (3D) survey and modelling allow us to digitally preserve the historical memory of such built heritage thanks to feasible, accurate, and portable tools and methodologies.

The development and refinement of 3D survey techniques, as well as their integration, involve the small objects, artistic and archaeological heritage, as well as many other types of cultural assets, sites, and landscapes. (Lerma et al., 2011, Remondino et al. 2014). With regard to museum assets, recent extensive digitalization projects aimed at achieving multilingual information archives that make digital libraries accessible to everyone. This is the main mission of Europeana project, but also of other institutions as the Getty Foundation or the Smithsonian institution, which are devoted to the preservation of Cultural Heritage (CH), promoting research, culture, and educational activities, or directing efforts towards the achievement of standards for CH and the realization of digital inventories.[1]

A first trend in techniques development aims to respond to the requests of the institutions, such as the museums that deal with conservation, arranging the massive detailed digitization of their preserved objects. About this, Hindmarch offers a very thorough research on the digitization of CH small assets, with a point of view that is centred on institutions requirements, such as museums (Hindmarch 2015), and an example currently much observed is the cultlab3D system (Santos et al., 2014). This trend is geared to the widespread use of 3D models, ranging from their possible use for further specialized studies to the acquisition and processing of virtual detailed copies that are as close as possible to the shape and contents of the real one. In this case, the models must be particularly dense and rich in information, with a very high accuracy and high geometrical and radiometric resolution. The first case study presented in paper falls into this first set of models and is applied to an Egyptian statue of the Archaeological Museum of Bologna, whose processed 3D model was subjected to Ultrasonic Tomographic Imaging (UTI) investigations (Di Pietra et al, 2017).

On the other hand, many museums look today for more interactive exhibitions that involve and increase the visitors' emotions enhancing the museum interactive experience (Kersten et al. 2017, Spanò et al., 2016). In recent years, in fact, museums' role changed from a mere "container" of cultural objects to a "narrative space" able to explain, describe, and revive the historical material

[1]   http://www.europeana.eu/portal/

http://www.getty.edu/about/whoweare/mission.htl

http://3d.si.edu/about

(Martina, 2014). The combination of these factors has contributed to the increase in the use of virtual reality and 3D models in museums installations that are offering to the visitors more dynamic and immersive experiences, and, in some cases, giving them the possibility to interact and select the information according to their interests. In this second scenario, 3D models must be suitably processed to make them easy to be handled by portable devices or even in web systems. In this case, the information density can decrease depending on the communication purpose, and, with the aim of maintaining high adhesion to the original object, the optimization of surfaces, involving remeshing techniques and textures maps, seems to be a very promising perspective.

The second case study of this paper is particularly connected to this study area. Two statues, known as "busti loricati of Susa" and representing two roman emperors, have been surveyed with a photogrammetric method with the aim to process two 3D models, representing the statues as they are now and as they were before the nineteenth century restoration, according to archive sources. Such models provided the base for a video installation for a museum, which simulates a holographic projection and explains the different armour parts highlighting them in sequence.

The structure of the article is as follows: in the next paragraph the employed methods for the 3D survey process are presented, together with the tested optimization techniques and the UTI method. Section 3 presents both case studies followed by conclusions and observations.

2. Methods Outline

2.1. 3D Survey Methods

In the field of ancient Cultural Heritage, 3D accurate models of archaeological objects and sculptures have a significant role for their documentation, maintenance, and restoration. The digitization of such heritage ensures the store of the information about the shape and appearance of an object against its possible lost and damage over time by natural or accidental causes. The collected data allow also the dissemination of digital media collections for a large audience via virtual museums and enable the creation of replicas via 3D prints.

In the last decade, the development in 3D survey techniques was rapid and continuous in producing new, more effective methods in terms of automation, acquisition, and processing speed, and the quality and precision of the output data. By now, it is well recognized that the integration of multisensor methods provide more complete and detailed data than standalone acquisition (Ramos et al., 2015; Trinks et al., 2017)

The employed sensors are generally distinguished in active and passive ones, basing on the emission of an electromagnetic signal.

Active sensors, as used in laser scanner (TOF) and range cameras (based on the triangulation principle), measure angles, and distances emitting signals (laser beams, infrared lights, etc.) and recording the reflected answers (Adami et al., 2015). The results of a laser scanner acquisition are point clouds that are constituted by millions of points, which can be coloured thanks to an integrated RGB camera, and from which it is possible to process very detailed textured 3D model and other two-dimensional (2D) more traditional representation. (Donadio et al., 2015).

Passive sensors, which are used in photogrammetric applications, use the ambient light to make measurements, recording the electromagnetic energy, i.e. visible light, emitted by the objects. In recent years, the development made on digital cameras and in calibration technology, in connection with very competitive costs, and especially thanks to the integration of *image matching* and *Structure from Motion* (SfM) algorithms, derived from the Computer Vision field, meant that photogrammetry is more and more used to recover objects with high accuracy (Samaan, et al. 2013). The final result is a dense 3D point cloud, which can be integrated with LiDAR data and processed to obtain a 3D textured model. In this process, it is also possible to generate true orthophotos in an increasingly automatic way, which are very useful metric products where radiometric information is combined with real measures allowing for a complete representation of the analysed object (Chiabrando et al., 2015). Such products are usable also as texture for mapping materials, deteriorations, or other important damaging effects. (Koska, et al., 2013; Rijsdijk, 2014).

In the very close range field, still among CH requirements, system such as the Time of Flight (ToF) cameras and structured light 3D scanners allow us to acquire with accuracies not lower than one or few millimetres. In the field of very high accuracy metrology systems (±25 ÷ 30μm), new developed scanning systems, such as arm scanners, combine arms together with high definition hand-held scanners. Such systems, even though they are still expensive, are very useful in rapid prototyping and reverse engineering fields.

To identify the most appropriate technology for 3D digitalization, several aspects must be considered:

- characteristics of the object (shape, dimension, colour, reflectivity and homogeneity of the material, etc.),
- the acquisition place (internally or externally, with natural or artificial light, with the possibility to move the object or not),
- the aim of the survey (documentation, analysis, dissemination, virtual reality applications, real time applications), and
- time and budget constraints.

In the following test cases, the statues have been surveyed by means of the photogrammetric technique, which allowed to pursue the level of detail requested by the UTI analysis and communication purposes. In addition, the Egyptian statue was also acquired by a hybrid hand-held Freestyle scanner, in order to test its potentialities and carry out some considerations concerning the quality of the acquired data in comparison to the photogrammetric ones.

2.2. 3D Model Optimization

As mentioned before, the modelling of object surfaces and points clouds produces detailed 3D models, consisting of millions of polygons and high resolution images, with very large data volumes, which are difficult to be handled and visualized by common computers, portable devices with low performance (e.g., Smartphones and tablets), or on the Internet. (Kersten et al., 2016). Despite technological developments, the management of large polygonal datasets is, in fact, influenced by several technical problems, i.e. very long processing and editing time or real-time visualization constrained by the graphics card performance (Manferdini and Remondino, 2012).

Nowadays, the scientific community is trying to find new ways to optimize and share such 3D digital contents, in order to guarantee fast access to the data and their effective communication (e.g., in dissemination and valorization application of Virtual and Augmented Reality), providing low resolution 3D models that are easy navigable and viewable (Guarnieri et al., 2010; Cipriani et al., 2017).

Some critical considerations about the contradiction between the great increase in digitization projects of cultural assets in the last decade and the problems that today are an obstacle to their massive sharing on the web can be found in Scopigno et al. (2017). They are attributable to intellectual property issues and of improper use fear, the confidentiality of ongoing projects, the recurring problem of scarcity of financial resources, and of high expertise required.

In all of the cases, it is necessary to establish the needs that the 3D model have to fulfill, which determine the final level of geometrical and radiometric accuracy, size, and visualization, but with the constant aim of not losing quality and information. Different purposes led to different processing choices and different optimization levels, depending on the final aim to pursue, whether it is a specialized analysis (Guidi et al., 2017), which require to maintain the geometric detail in the final mesh or a communication application, which needs a lower data volume (Kai-Browne et al., 2016).

To achieve this, various methods that were borrowed from the field of gaming technology can be employed for drastically reducing the file size while maintaining a very high degree of detail. Game engine and entertainment software, in fact, provide several useful tools to process and generate Low Poly models, which show however a good detail on the surfaces in a very low byte files.

The whole process of computing, given a 3D mesh, a new mesh whose elements satisfy some quality requirements, while approximating the input acceptably, is called "re-meshing" (Alliez et al., 2008).

Among the available tools of the remeshing we mention the decimation and retopology algorithms, the SubDivision surfaces, and Polynomial texture maps (PTM). The decimation module automatically decreases the number of faces in the model, deleting the vertices depending on the specific decimation ratio as specified by the user. The retopology technique, which requires a skilled and experienced operator, consists in manually tracing the High Poly mesh with a square mesh of lower density, called "quad-dominant mesh". The final quadrangular mesh can support the conversion into Catmull-Clark SubDivision surface, which is a variable-detail model that may be interactively increased in different output scales by adjusting the level of subdivision (Merlo et al., 2013)

PTM is an image-based relighting technique for visualizing the appearance of surface under variable lighting condition. Pan et al. (2016) diffuse color maps, normal maps, and displacement maps are some examples. In order to compute such 2D representation, it is essential to firstly process the UV map of each 3D model by unwrapping it in a 2D coordinate system (u, v), which ensures the spatial link between the x, y, z coordinates of the mesh polygons and the image. After the UV mapping different textures can be computed, projecting surface information from the high resolution mesh onto the Low Poly mesh, converting geometrical characteristics into pixel information in a so-called baking process.

A normal map, for example, contains the surface normal vector of the high-resolution mesh, which is stored as a RGB value in the pixel image. Once calculated and applied to the Low-poly mesh, the normal map simulates the behavior of light reflections from the starting model, adjusting the shading of the low-detail model, which looks again like the original Hi-poly model.

The displacement map is, instead, a grey scale image, in which each shade of grey stands for a deviation of the background mesh from the optimized one. This is because, unlike the normal map, the displacement map, once applied to the model, displaces the points of the Low-poly mesh basing on the deviations calculated in the baking process (Merlo et al., 2013)

In this paper, the optimization process has been realized within the software: 3DReshaper, MeshLab, and Blender.3D Reshaper was used for the mesh generation from the points clouds. MeshLab was chosen for the effectiveness of its tools for mesh editing, cleaning and remeshing whereas Blender was chosen due to its capabilities in re-meshing, UV unwrapping, and baking.

2.3. UTI Method

Micro geophysics techniques can contribute to facilitating the restoration of artworks or historical building elements, also evaluating, with respect to the

management of a museum, the possibility and the precautions that must be taken when moving artefacts (Piro et al., 2015).

The 3D Ultrasonic Tomographic Imaging (UTI) method consists in the estimation of the variation of the apparent velocity of an ultrasonic (US) pulse send within the volume of interest (VOI) (e.g., Sambuelli et al., 2015). According to the theory of elasticity, in fact, the velocity of propagation of a mechanical pulse in a given material decrease, for example, with the increasing of the number of fracture in unit of volume. It is estimated that dividing the Euclidean distance d between a transmitter probe, TX, and a receiver probe, RX, by the shortest time t (time break - TB) that the US impulse need to travel from TX to RX. This velocity is called apparent because the US pulse does not really travel through the low velocity volume (Wieland, 1987), but rather, according to the Fermat principle, it travels around it, taking a longer time. Dividing the straight path by a longer time we get a lower velocity, and this is the sign that between TX and RX there is an inhomogeneity, which can be due to the presence of weaker volume of rock, mortar, or a more densely fractured medium.

3. Experiments

3.1. Case Study 1: Integrated Investigations on a Damaged Egyptian Statue

The work aimed at highlighting the ability of methods that are devoted to the 3D geometry acquisition of small objects when applied to diagnosis performed by geophysical investigation (Figure 1). The data acquisition consisted in a photogrammetric survey and in two type of laser scanner: a laser Faro Focus 3D and the hybrid hand-held Freestyle scanner, in order to carry out some considerations concerning the quality of the acquired data in relation also to the Ultrasonic Tomographic analysis needs (Di Pietra et al., 2017). Since the statue was in a laboratory, with a bad light condition, we decided to add some artificial properly oriented lights.

3.1.1. The Egyptian Naophorous Statue of Amenmes and Reshpu

The survey is applied to the Egyptian *naophorous* statue of Amenmes and Reshpu, which dates to the reign of Ramses II (1279-1213 BC) or later, and is now preserved in the Civic Archaeological Museum in Bologna (Inv. no. MCABo EG 1821) (Kminek-Szedlo, 1895). The statue was dedicated to the gods Osiris, Isis, and Horus by two high officials of the Amun temple in Thebes, Amenmes and Reshpu.

The statue presents a worrying deterioration of its limestone, consisting in stone material chips and cracks, especially on the inscribed base. In order to interrupt the increasingly rapid and progressive deterioration, and to clean and

consolidate the limestone, the Civic Archaeological Museum has sought the cooperation of prestigious Italian institutions and a restorer expert in stone conservation [2] (Picchi, 2016).

Figure 1. (**Left**) Worrying state of deterioration of the statue with visible fractures, (**right**) the ultrasonic measurements to reconstruct the fracturing state of the statue needs to know several vector size between points on the damaged surface.

3.1.2. The Integrated 3D Survey Technique

The survey phase consisted in a photogrammetric and laser acquisition of the statue, with the aim to generate a 3D model, on which it can make a variety of detailed 3D measures. In particular, it was necessary to evaluate on the processed 3D model the locations of the source and receiver points of the Ultrasonic Tomographic test, their coordinates in a fixed reference system, and their mutual distance. Before any acquisition, eight checkerboard targets have been placed on the base of the statue, to be used for registering all of the data in a unique reference system, and 71 white numbered stickers have been arranged on the statue to form a 3D network of max $150 \times 150 \times 150$ mm^3/voxler, as a 3D mesh for ultrasonic tomography (Figure 1).

The photogrammetric survey consisted in the acquisition of 74 images, captured at three different heights all around the object with a Nikon D800E (7360×4912 CMOS sensor, Zeiss optic system and 50 mm focal length) at a distance of 1 m. The acquired images have been processed by means of the Structure from Motion (SfM) technique and image matching algorithms, thus generating a dense point cloud that is constituted by some six mil. points. The high quality of the bundle adjustment process was secured by the re-projection error limited to 1.2 pixel. After these steps, a reference system has been assigned to the

---

[2]   Engel (*Environmental-Engineering Geophysics Laboratory*) and Geomatics Laboratory of Politecnico in Turin, Opificio delle Pietre Dure (OPD) in Florence, IUAV University in Venice and the restorer Cristina Del Gallo.

point cloud, scaling also the model according to measures between targets placed on the crankcase. The targets positions have been obtained by the terrestrial fixed scanning (Faro Focus 3D scanner, featured by measurement accuracy of ±2mm up to 10m), which is specially used to make the photogrammetric model that is independent from the next one generated by the freestyle hybrid scanner. Subsequently, a textured 3D model has been processed, ensuring an average accuracy on the final model of less than 2 mm (accuracy evaluated measuring some control points on the mesh and on the original point cloud) (Figure 2).

The second step of the survey test applied to the statue employed a handheld 3D laser scanning (the FARO Scanner Freestyle3D: http://www.faro.com/products/ 3d-documentation/faro-scanner-freestyle-3d/overview).

Such an instrument offers fast data acquisition and real-time visualisation; it uses a structured light technology consisting in two infrared cameras that create a "stereo pair" of images that are looking at the structured light pattern, which allows for the determination of the moving centre. A laser sensor ensures the measurement of the surveyed surface with a range of acquisition of 0.5-3 m, (3D point accuracy 1.5 mm) and an RGB camera acquires the radiometric data. Its relatively low cost makes such technique suitable and reliable for small objects modelling and addressable for many different uses. The acquisition phase consisted in five scans collected at a distance from the object of 0.5 m, providing a resolution of 0.2 mm and with a predicted noise of 0.7 mm. Certainly, the ambient light is a determining factor for the accuracy of the clouds, and, in fact, the registration process that is based on the automatic target recognition ended with an average residual of 2–3 mm, which is insufficient for the intended purposes. The final point cloud, obtained after a progressive alignment according to the shape of clouds, is constituted by some nine mil points. The amount of cloud points refers to the exact surface extension used for the photogrammetric model so as to give value to the comparison of the clouds.

One of the aim of the work was the evaluation of the accuracy of both the surveys, mostly regarding the possibility for the freestyle laser point cloud to provide a sufficient level of detail for the Ultrasonic Tomographic needs. As reported in Table 1, the laser Freestyle cloud is constituted by a highest number of points than the photogrammetric one. The roughness of both the points clouds has been computed in Cloud Compare, which estimates the distance between each point and the best fitting surface computed on its nearest neighbours. As shown in Figure 3 and Table 1, the photogrammetric cloud has minimal noise with a mean value of 0.269 mm, while the freestyle cloud presents a higher noise, with a mean value of 0.552 mm (to make such estimation a radius of a sphere centred on each point of 0.005 m has been considered) (Figure 3). Once aligned, several section profiles have been also extracted from both the cloud. Measuring samples of residuals among the photogrammetric cloud, assumed as the reference cloud, and

the freestyle one, we have been able to estimate that the second one has discards of 1–2 mm due to alignment operation and its roughness. As it is possible to notice in Figure 4, we also computed the level of points density: the freestyle cloud has a higher number of points and a higher density, but the points distribution is less uniform (to make such estimation a radius of a sphere centred on each point of 0.01 m has been considered). This is due surely to the acquisition process related to the operator motion.

Figure 2. Photogrammetric point cloud, mesh and textured mesh.
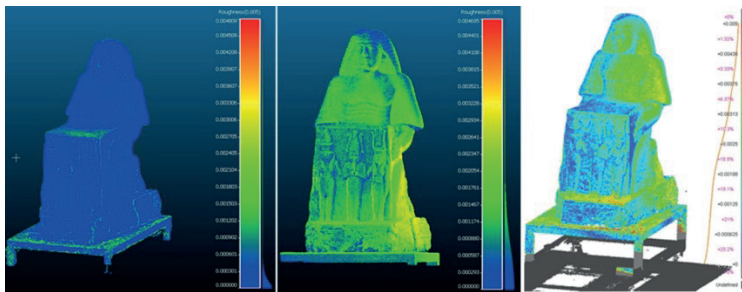
Figure 3. Evaluation of the level of roughness of the clouds; (**left**) insignificant level of roughness computed on the photogrammetric cloud (less than 0.5 mm almost throughout the cloud); (**middle**) laser cloud presenting a higher percentage of points affected by noise (several at 2.5–3 mm); comparison between clouds (**right**) about 60% of the freestyle point cloud is at a distance of less than 2 m from the photogrammetric cloud.
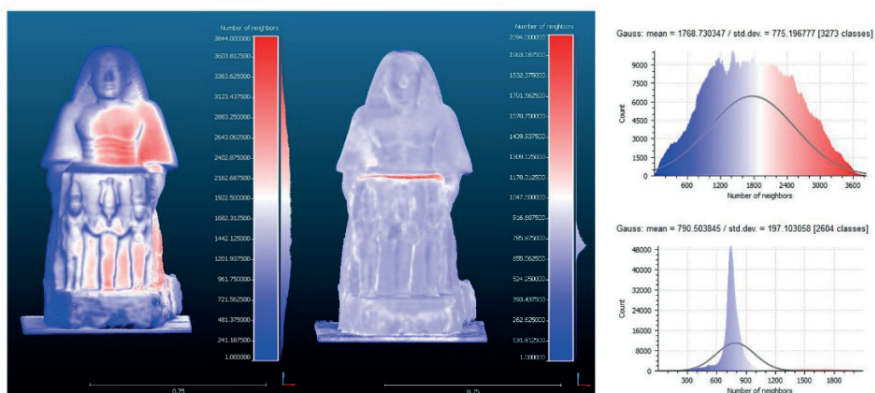
Figure 4. Points density: freestyle cloud (**left**); photogrammetric cloud (**middle**); histogram distribution of the points density - freestyle cloud (**right above**); histogram distribution of the points density – photogrammetric cloud (**right below**).

Table 1. Number of points, level of roughness and level of points density computed in both the clouds in Cloud Compare.

	Number of Points	Roughness Mean Value	Density Mean Value (in a Spherical Neighbourhood with Radius of 0.01 m)	Std. Dev.
Photogrammetric data	6.011.037	0.269 mm	790 points	197 points
Laser Freestyle data	9.195.056	0.552 mm	1768 points	775 points

3.1.3. UTI Data Acquisition and Processing

The 3D UTI on Amenmes was restricted to the lower part of the statue, which was the part giving major concern about its mechanical properties. Around this volume, 71 points have been materialized with sticky circular stamps (diameter 15 mm), on which the central point and a progressive number were marked (Figure 1).

The point positions were planned so that, on average, the straight rays connecting each couple of points would have crossed the VOI with a dense 3D net and would have not left volumes greater than 15 × 15 × 15 cm not scanned. To acquire, store and process the geophysical data the following instruments and software's were used. A PUNDIT pulse generator with exponential US probes with a nominal frequency of 50 kHz; a 7 dB fixed gain amplifier, a variable gain (1, 3, 10 dB) amplifier; a Le Croy Wave Jet 20 MHz digital oscilloscope; Matlab proprietary scripts for time reading, straight rays tracing and velocity interpolation; and, the software GeoTomCG by GeoTom LLC for 3D UTI and the

software Voxler by Golden Software for 3D rendering of the velocity volumes. Across the VOI, 226 measurements were made according to the scheme in Figure 6, right. Before the measurements, the time delay introduced by the exponential probes was measured and it was 20.7 µs. This time was subtracted from each TB. In Figure 5 (left), an example of the graph on which the TB's were read is shown.
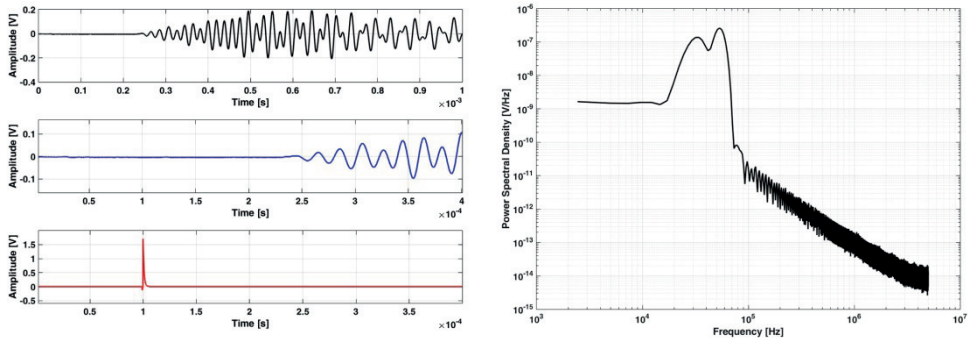

Figure 5. Top raw ultrasonic (US) signal (**left above**); zoomed US signal to read the TB (**left center**); triggering signal from which the time-zero (the time the US pulse entered the rock) was read (**left below**); PSD of a transmitted US pulse (**right**).

The spatial resolution, i.e., the smaller detectable anomalous volume, of a 3D UTI is roughly related to the dominant wavelength λ of the US pulse. An estimation of λ can be obtained dividing, for example, the average velocity of US pulse in the medium by the dominant frequency of the US pulse itself. To evaluate an order of magnitude of the achievable spatial resolution in the 3D UTI, the power spectral density (PSD) of some long-path and short-path signals have been evaluated. The PSD graph, as shown in Figure 5 (right), can be considered as representative of most of the transmitted signals. From the graph, the main energy content is roughly within 30 and 60 kHz.

When considering an uncertainty on d equal to 5 mm and on t equal to 15 µs, an uncertainty of 60 m/s can be supposed on apparent velocities. An elementary statistical analysis on the apparent velocities gives: minimum velocity 300 m/s (this value is not realistic and it's likely due to a missing FB); maximum velocity 2800 m/s; mean velocity 1330 ± 60 m/s; velocity standard deviation 630 m/s. From the velocity values and the PSD frequency band, a dominant wavelength of 5 cm could be safely assumed. In Figure 6 (left) a histogram of the apparent velocities is shown. The histogram clearly shows that many apparent velocities are around and even below 1000 m/s; that is a quite low velocity range for a limestone. In figure 6 (middle) a plot of d versus TB is shown.
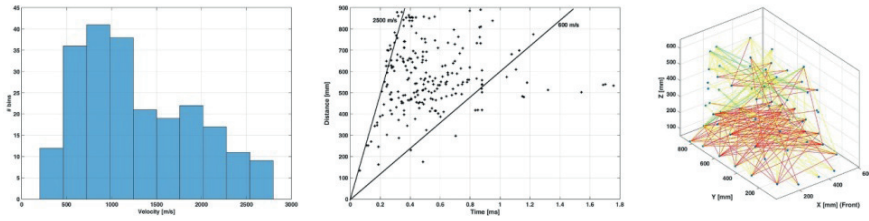
Figure 6. Histogram of the apparent velocities (**left**); distance d versus Time TB plot (**center**); the Euclidean straight paths used in three-dimensional (3D) Ultrasonic Tomographic Imaging (UTI) processing. Ray colour codes refer to apparent velocities: red v < 1300 m/s; yellow 1300 < v < 2500 m/s; green v > 2500 m/s (**right**).

The slope of each straight line on the graph in Figure 6 (middle) is an apparent velocity. The two continuous lines represents two velocities. The points relative to a sound limestone should lie around or above the line at 2500 m/s. This graph shows that within the VOI, a few rays have an apparent velocity that is compatible with a sound limestone.

In Figure 6 (right), a 3D view of the straight ray paths used in the 3D UTI is shown. Each ray path is drawn with a colour related to its apparent velocity. Even in this representation, before the 3D UTI processing, it is easy to guess that the lower part of the statue has worse mechanical properties than the higher part.

3.1.4. 3D UTI and Improved Graphical Representation

UTI analysis has been performed with the software GeoTomCG (by GeoTom, LLC, http://dev.geotom.net), which allows for the tomographic processing of seismic data in a volume with sources and receivers located anywhere on a 3D Cartesian grid. GeoTomCG uses a SIRT (Simultaneous Iterative Reconstruction Tomography) algorithm to produce, from the position (x, y, z) of transmitters and receivers and from the TB's, a velocity distribution in the VOI (Trampert and Leveque, 1990). The volume is firstly discretized in prismatic cells, and then an iterative procedure is used to calculate the velocity of the US pulse within each cell. The VOI of Amenmes was discretized in 5 × 8 × 6 prismatic cells with size: dx = 114 mm, dy = 108 mm, dz = 101 mm. Then, on average, the cell size was about two times the dominant wavelength of the US pulse along each direction. From the final model, only the cells crossed by more than three rays have been considered, and a 3D rendering of the resulting velocity distribution has been plotted.

From the 3D UTI analysis, it is possible to extract a standard file format that typically used in computational fluid dynamics (CFD), the PLOT3D file. It is a standard format that usually includes two different files, the grid file and the

solution file. The first contains the coordinate of the solution grid, while the second contains information typical of a CFD solution, in our case, the correspondent velocities. With the aim to improve the visualization of the results of the 3D UTI analysis and to make volumetric measurements on the statue, the PLOT3D file format has been converted in a standard format that is usable in a 3D point cloud processing software. In particular, an easy function, developed in Matlab was used to transform the structure of the grid file in a .xyz file, where the coordinate of the grid could be visualized as a sparse point cloud and the velocity value as a scale bar. The VOI of Amenmes extracted from GeoTomCG software was discretize in $30 \times 45 \times 35$ prismatic cells with size of 20 mm. The correspondent point cloud that was extracted with Matlab was too sparse so it was oversampled with the use of the Point Cloud Library (PCL), an open project (Rusu, Cousins, 2011), integrated as plugin in the open source software Cloud Compare. The tool 'Smoothing MLS' allows to interpolate the point cloud with the moving last square method so that the initial cloud can move from 47.250 to 37.469.250 points. At the end of the process, it has obtained a 3D representation of the velocity distribution in the VOI of Amenmes statue. The graphical representation was like the one already used in the UTI analysis with: red colour v < 1500 m/s, yellow 1501 < v < 2000 m/s, green 2001 < v < 2500 m/s, dark green 2501 < v < 3000 m/s, and blue v > 3001 m/s. The VOI represented with this scale bar, was combined with the statue points cloud and this has made possible the representation of different section level to better understand the region that was affected by anomalies (Figure 7, left).

The iso-surface was created, extrapolating the points of the cloud belonging to the separation surface between the velocity defined before, and generating the corresponding mesh. Once defined, the iso-surfaces and the points cloud between two steps level, it was possible to compute the volume of statue for each average velocity, and so the volume was characterized by the worse mechanical proprieties. The volumes were defined from a meshed closed shell that was generated with the portion of points cloud included between two iso-surfaces and was measured with the tool Measure/Volume of the software 3DReshaper (Figure 7, right – Table 2).

Table 2. The volumes of the statue for each range of velocity.

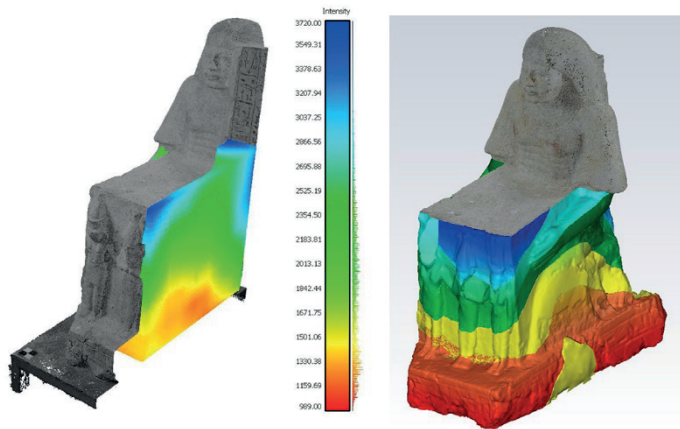| Average Velocities [m/s]	Interested Volumes [m³]	Percentage Compared to Investigated Volume [%]
v < 1500	0.077 m^3	38.31%
1500 < v < 2000	0.053 m^3	26.37%
2000 < v < 2500	0.039 m^3	19.40%
2500 < v < 3000	0.025 m^3	12.44%
V > 3000	0.007 m^3	3.48%

Figure 7. Improved representation of average velocities in the VOI of the Ramessid statue and the closed mesh extracted from the classified point cloud.

In conclusion, the survey applied to the Egyptian sculpture proved that a little less than 40% of the volume of the crankcase presents a state of conservation particularly worrying (Table 2), since the overall measured average velocity is lower than 1500 m/s, due to damages and fractures.

3.2. Case Study 2: Optimization Surface Methods on a Roman Statue for Communicative Purpose

The second case study is aimed at the dissemination of an archeological asset producing multimedia contents from multi-sensor surveyed 3D data.

3.2.1. The Roman Loricate Busts of Susa

The ruins of the two "loricati" busts (so named because of the decorated armour), representing two Julio-Claudians emperor, (Figure 8) were found in 1802 in the city of Susa and in the nineteenth century a restoration action completed them adding the missing heads, low parts of the legs, and the arms.

These busts and their decorated armours are an exceptional witness of the north Italian sculpture during the first imperial age (Cadario, 2005). In the first bust, the decoration invokes the mythical origins of the *gens Iulia* (Figure 8, left), whereas in the second *torso* (Figure 8, right), the representation had to summon the victory against Middle East areas after the Parti population' submission. (Cadario, 2005).

Figure 8. The roman statues placed inside the Civic Archaeological Museum in Turin.

3.2.2. The Photogrammetric Survey

The aim of the 3D survey was to process two detailed textured models of the busts, as they are today and the way they were before the addition of the nineteenth century restoration, to be used for a multimedia installation in the new Civic Museum of Susa.

Both of the statues have been surveyed by means of a photogrammetric application with a Canon EOS-1Ds Mark II with a 50 mm focal length. About 200 images have been captured at three different heights all around the statues at a distance of about 1 m and processed by means of the Structure from Motion (SfM) technique and image matching algorithms. After the image alignment, a dense point cloud constituted by about 12 mil. (bust with the baldric) and 15 mil. (bust without the baldric) of points have been generated, as well as a 3D mesh model of about 2.5 mil. and 3.4 mil. triangles, textured with the images acquired. After these steps, the data have been scaled according to measures taken between targets placed in the scene. The surface resolution was very high, respectively, of 0.253mm/pix and 0.221mm/pix (Figure 9).

3.2.3. The Bust 1: 3D Models Optimization

In the optimization process, we tested several decimation and remeshing tools in order to make some evaluation on different levels of decimation, by comparing the geometrical accuracy that was preserved and the byte of the output files. This test was also suggested by the final use of the 3D models which was a multimedia installation for the Museum.

A first step of the optimization was done within the software Photoscan where the 3D model has been generated.

Even though the parameters for the mesh processing were set very high and with the interpolation disabled, the mesh presented a bad topology, especially in the arm and the neck part (Figure 9).
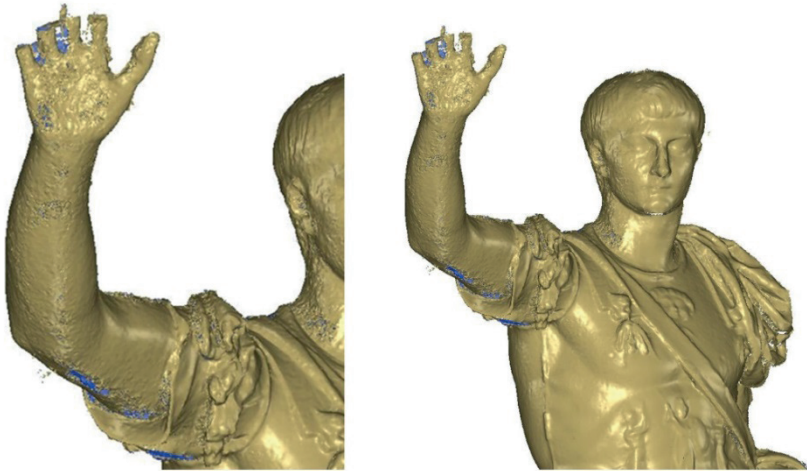

Figure 9. Mesh processed in Photoscan; it is possible to notice the topological error that affect the surface.

For these reasons, we decimated the mesh with the Photoscan tools from 2.457.747 triangles to 1.800.000 triangles (a lower number made the mesh too smoothed), and we also ran the command "Fix Topology", which is active if there are any topological problems and can be clicked to solve the problems (Figure 10).
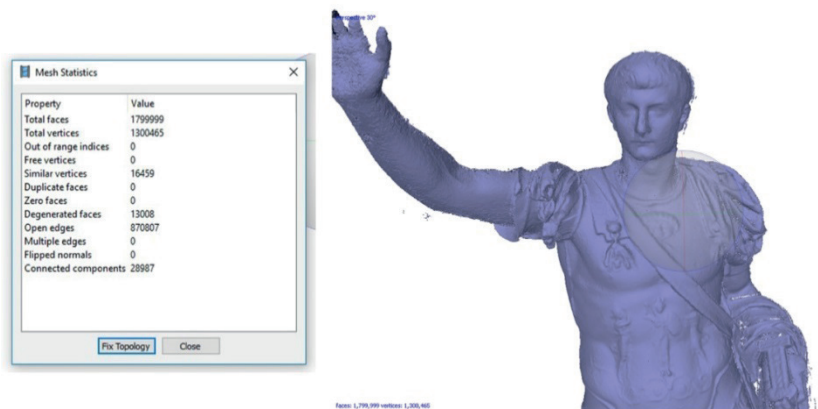

Figure 10. Mesh after the decimation filter to 1.800.000 faces.

Since the mesh so decimated did not satisfy the geometrical requests, due to the continued presence of noise, we decided to make a new one exporting the dense point cloud within the software 3D Reshaper.

The mesh has been processed in 3D Reshaper setting a triangle size of 0.003 m and refining it taking new points from the cloud with a deviation error of 0.002 m. In Figure 11 and in Table 3, it is possible to notice that the final mesh has a greater quality when compared to the Photoscan ones, a very good geometrical detail, fewer topological errors and also a lower byte file.

Table 3. Comparison between the mesh computed within the photogrammetric software and the one realized from the photogrammetric cloud in 3D Reshaper.

	N. Points	N. Triangles	N. of Independent Pieces	N. of Holes or Free Contours	KB File .obj.
Mesh Photoscan	1.720.221	2.457.747	30.405	71.075	110.309
Mesh 3DReshaper	374.774	741.327	2	264	37.390

Figure 11. Original high detail mesh model processed in 3D Reshaper.

In order to process, as mentioned before, an extreme optimization of the model, testing the potentialities of the remeshing tools, we imported the model in MeshLab in order to test several levels of decimation.

After the application of the filters of cleaning and repairing, which allow us to remove duplicate faces and vertices, non manifold edges and vertices, we ran the

command *Simplification: Quadric Edge Collapse Decimation* to reduce the number of vertices setting the minimum number of faces of the final remeshed mesh.

In order to identify different steps of decimation, which can respond to different purposes, we tested and compared three type of decimation and optimization (Figures 12 and 13, Table 4):

- In a first level, the mesh is decimated indiscriminately and automatically with the *Quadric Edge Collapse Decimation* tool. In this process, it is not possible to reduce that much the mesh if you do not want to completely lose the geometric and visible detail. For this reason, we set the decimation from 741.327 to 100.000 faces. The file size changed from 37.390 KB to 2.483 KB, but visually the mesh still has a good level of detail, although it is more smoothed (Figure 12, left).
- In a second level, we tried to maintain the original high level of detail in the high detailed portions (the decorated armour and the *pterigi* part), hardly decimating just the flat part, such as the legs and the arm. In this way, the file size is reduced a little less but the detail on the decorated portion is still very high. (Figure 12, middle–right).
- In the third level of optimization, we tried to reduce at most the mesh making use of the Polynomial texture maps (PTM) to just visually simulate the detail. The mesh has been decimated to 7000 faces and then imported in Blender for the UV mapping and baking process. In order to minimize the work time, we used the UV map that was automatically generated by the unwrapping tool and then we calculate the UV map, also importing the original High Poly mesh. The final result is a 3D model that looks like the original one but with a very low size in terms of byte. This representation is very suitable for entertainment application, such as the one aimed for the museum, but it is important to highlight that it has completely lost its geometric detail, making it useless for other kind of specialized geometrical analysis (Figure 13).
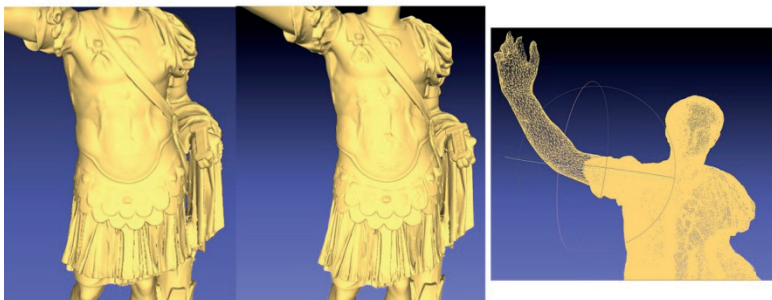

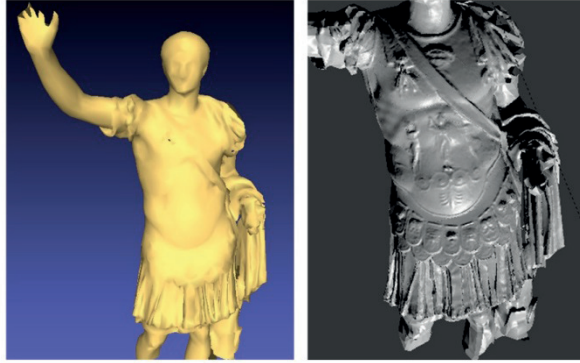**Figure 12.** Level 1: decimated surface mesh; Level 2: surface model and wireframe view.

Figure 13. Level 3: Decimated mesh before and after the projection of the Normal Map calculated in Blender.

Table 4. Comparison between different optimization level.

	N. Vertices	N. of Faces	KB file .obj	% KB Reduction	% Faces Reduction
Original mesh	374.774	741.327	37.390	-	-
Level 1	52.622	100.000	8.599	77%	86,5%
Level 2	147.754	288.165	25.200	32,6%	61%
Level 3	3.874	7.000	575	98%	99%

4. Conclusions

As shown in this article, Cultural Heritage assets can have great benefits from 3D data and reality-based models for multipurpose aims. It is possible to outline different considerations pertaining the cases study and the methods.

The survey applied to the Egyptian sculpture prove that a little less than 40% of the volume of the crankcase presents a state of conservation that is particularly worrying (Table 2), since the overall measured average velocity is lower than 1500 m/s, due to damages and fractures. That means that the integration of the two methods is capable of investigating the magnitude of the internal damage of stone objects, which is a necessity that is encountered in most cases of cultural heritage and small objects too.

The operative outcomes of the second application are summarized in Table 4: the conclusion of the optimization process leads to having a model reduced by 99% with respect to the original one, which is therefore more suitable for communication projects that require good perception, even though it may be not featured by high level of geometric resolution and accuracy.

In the field of methods evaluation, the versatility of the photogrammetric survey, after the development of the SfM technique, is more than established,

although it must be considered that to obtain high accuracies, such as those achieved in the presented test cases, high-quality cameras and optics must be available and a high level of expertise in the modelling phase is necessary. When compared to the most popular and tested hand-held Kinect scanner, the Faro Freestyle present advantages that may make it attractive in cultural heritage documentation: it is portable, it provides full colour point clouds, it is easy to use and is versatile, reaching the extension of small rooms survey, and it is cheaper than many other systems.

Concerning the UTI test, in addition to the proof of the possibility for the processed 3D models to provide useful detailed data, the improvement of the graphic representation of the results is another key result. On this point, it is necessary to highlight that we met many difficulties in the interoperability of digital data formats and many operations and transformations of formats were made with laborious manual processes.

With the optimization methods that are involved in the second test case, we proved how reality-based 3D modelling methodologies might satisfy the requests of dissemination, sharing, and access of Cultural Heritage information. Innovative digital applications provide great potentialities for institutions and museums in helping them to preserve heritage, ensuring the ability to reach multimedia contents with educational purposes, and then to promote themselves. Digital contents accessible time and location independently, immersive experiences, and virtual visits represent new methodologies to increase the communication and transmission of culture, today and into the future generations. Pursuing this aim, we proved how procedures borrowed from reverse modelling and mapping allow us to generate extremely precise visualization, with a very low computing cost.

References

1. Adami, A.; Balletti, C.; Fassi, F.; Fregonese, L.; Guerra, F.; Taffurelli, L.; Vernier, P. The bust of Francesco II Gonzaga: From digital documentation to 3d printing. *ISPRS Ann. Photogramm. Remote Sens. Spat. Inf. Sci.* **2015**, *2*, doi:10.5194/isprsannals-II-5-W3-9-2015.

2. Alliez, P.; Ucelli, G.; Gotsman, C.; Attene, M. Recent advances in remeshing of surfaces. In *Shape Analysis and Structuring*; Springer: Berlin/Heidelberg, Germany, 2008; pp. 53–82, doi:10.1007/978-3-540-33265-7_2.

3. Cadario, M. Ipotesi sulla circolazione dell'immagine loricata in età imperiale: I torsi giulio-claudi di Susa. In La Scultura Romana Dell'italia Settentrionale. Quarant'anni Dopo la Mostra di Bologna. Atti del Convegno Internazionale di Studi. Pavia, 22–23 September 2005; Slavazzi, F., Maggi, S., Eds.; All'Insegna del Giglio: Firenze, Italy, 2005.

4. Campana, S. 3D Modelling in Archaeology and Cultural Heritage. Theory and Best Practices. In *3D Recording and Modelling in Archaeology and Cultural Heritage. Theory and Best Practices: Archaelogical Needs*; Remondino, F., Campana, S., Eds.; BAR International Series 2598; Archaeopress: Oxford, UK, 2014; pp. 7–12.

5. Cipriani, L.; Fantini, F. Digitalization Culture VS Archaeological Visualization: Integration of Pipelines and Open Issues. *Int. Arch. Photogramm. Remote Sens. Spat. Inf. Sci.* **2017**, *42-2(W3)*, 195–202, doi:10.5194/isprs-archives-XLII-2-W3-195-2017.

6. Chiabrando, F.; Donadio, E.; Fernandez-Palacios, B.; Remondino, F.; Spanò, A. Modelli 3D multisensore per l'acropoli segusina. In *L'arco di Susa e i Monumenti Della Propaganda Imperiale in età Augustea*; Del Vecchio, P., Eds.; Susa, Italy, 2015; pp. 217–232.

7. Di Pietra, V.; Donadio, E.; Picchi, D.; Sambuelli, L.; Spanò, A. Multi-source 3d models supporting ultrasonic test to investigate an egyptian sculpture of the archaeological museum in Bologna. *Int. Arch. Photogramm. Remote Sens. Spatial Inf. Sci.* **2017**, *XLII-2/W3*, 259–266, doi:10.5194/isprs-archives-XLII-2-W3-259-2017.

8. Donadio, E.; Chiabrando, F.; Sammartano, G.; Spanò, A. Reality Based Modeling Training. Photomodelling and LiDAR Techniques for the St. Uberto Church in Venaria Reale. In Proceedings of the Disegno & Città, Torino, Italy, 17–19 settembre 2015.

9. Gonizzi Barsanti, S.; Guidi, G. A Geometric Processing Workflow for Transforming Reality-Based 3d Models in Volumetric Meshes Suitable for Fea. *Int. Arch. Photogramm. Remote Sens. Spatial Inf. Sci.* **2017**, *XLII-W3*, 331–338, doi:10.5194/isprs-archives-XLII-2-W3-331-2017.

10. Guarnieri, A.; Pirotti, F.; Vettore, A. Cultural heritage interactive 3D models on the web: An approach using open source and free software, *J. Cult. Heritage* **2010**, *11*, 350–353, doi:10.1016/j.culher.2009.11.011.

11. Hindmarch, J. Investigating the Use of 3D Digitisation for Public Facing Applications in Cultural Heritage Institutions. Ph.D. Thesis, University College London, London, UK, 2016.

12. Kai-Browne, A.; Kohlmeyer, K.; Gonnella, J.; Bremer, T.; Brandhorst, S.; Balda, F.; Plesch, S.; Lehmann, D. 3D Acquisition, Processing and Visualization of Archaeological Artifacts. In Proceedings of the Euro-Mediterranean Conference, Nicosia, Cyprus, 31 October–5 November 2016; Springer International Publishing: Berlin, Germany, 2016; pp. 397–408, doi:10.1007/978-3-319-48496-9_32.

13. Kersten, T.P.; Lindstaedt, M. Potential of Automatic 3D object reconstruction from multiple Images for applications in Architecture, Cultural Heritage and Archaeology. *Int. J. Heritage Digit. Era Multi. Sci. Publ.* **2012**, *1*, 399–420, doi:10.1260/2047-4970-1.3.399.

14. Kersten, T.P.; Hinrichsen, N.; Lindstaedt, M.; Weber, C.; Schreyer, K.; Tschirschwitz, F. Architectural Historical 4D Documentation of the Old-Segeberg Town House by Photogrammetry, Terrestrial Laser Scanning and Historical Analysis. In Proceedings of the Euro-Mediterranean Conference, Limassol, Cyprus, 3–8 November 2014, Springer International Publishing: Berlin, Germany, 2014; pp. 35–47, doi:10.1007/978-3-319-13695-0_4.

15. Kersten, T.P.; Omelanowsky, D.; Lindstaedt, M. Investigations of Low-Cost Systems for 3D Reconstruction of Small Objects. In Proceedings of the Euro-Mediterranean Conference, Nicosia, Cyprus, 31 October–5 November 2016, Springer International Publishing: Berlin, Germany, 2016; pp. 521–532, doi:10.1007/978-3-319-48496-9_41.

16. Kersten, T.P.; Tschirschwitz, F.; Deggim, S. Developement of a virtual museum including a 4D presentation of building history in virtual reality. *Int. Arch. Photogramm. Remote Sens. Spatial Inf. Sci.* **2017**, *42-2(W3)*, 361–367, doi:10.5194/isprs-archives-XLII-2-W3-361-2017.

17. Museo Civico; Kminek-Szedlo, G. *Museo Civico di Bologna: Catalogo di Antichità Egizie*; Stamp. Reale Della Ditta G. B. Paravia e C. Edit.: Turin, Italy, 1895.

18. Kyriakaki, G.; Doulamis, A.; Doulamis, N.; Ioannides, M.; Makantasis, K.; Protopapadakis, E.; Hadjiprocopis, A.; Wenzel, K.; Fritsch, D.; Klein, M.; et al. 4D Reconstruction of Tangible Cultural Heritage Objects from Web-Retrieved mages. *Int. J. Heritage Digital Era* **2014**, *3*, 431–452, doi:10.1260/2047-4970.3.2.431.

19. Lerma, J.L.; Navarro, S.; Cabrelles, M.; Villaverde, V. Terrestrial laser scanning and close range photogrammetry for 3D archaeological documentation: The Upper Palaeolithic Cave of Parpalló as a case study. *J. Arch. Sci.* **2010**, *37*, 499–507, doi:10.1016/j.jas.2009.10.011.

20. Manferdini, A.M.; Remondino, F. A review of reality-based 3D model generation, segmentation and web-based visualization methods. *Int. J. Heritage Digital Era* **2012**, *1*, 103–123, doi:10.1260/2047-4970.1.1.103.

21. Martina, A. Virtual Heritage: New Technologies for Edutainment. Ph.D. Thesis, Politecnico di Torino, Torino, Italy, 2014.

22. Merlo, A.; Fantini, F.; Lavoratti, G.; Aliperta, A.; Hernández, J.L. Texturing e ottimizzazione dei modelli digitali reality based: La chiesa della Compañía de Jesús. *DisegnareCon* **2013**, *6*, 1–14.

23. Pan, R.; Tang, Z.; Xu, S.; Da, W. Normals and texture fusion for enhancing orthogonal projections of 3D models. *J. Cult. Heritage* **2017**, *23*, 33–39, doi:10.1016/j.culher.2016.07.009.

24. Picchi, D. Statua naofora di Amenmes e Reshpu. In *Restituzioni 2016. Tesori d'arte Restaurati*; Bertelli, G., Bonsanti, G., Eds.; Exhibition cataloque, Milan 1 April–17 July 2016; Marsilio: Venezia, Italy, 2016; pp. 30–37.

25. Piro, S.; Negri, S.; Quarta, T.A.M.; Pipan, M.; Forte, E.; Ciminale, M.; Cardarelli, E.; Capizzi, P.; Sambuelli, L. Geophysics and cultural heritage: A living field of research for Italian geophysicists. *First Break* **2015**, *33*, 43–54.

26. Remondino, F.; Spera, M.G.; Nocerino, E.; Menna, F.; Nex, F. State of the art in high density image matching. *Photogramm. Rec.* **2014**, *29*, 144–166, doi:10.1111/phor.12063.

27. Rusu, R.B.; Cousins, S. 3D is here: Point Cloud Library (PCL). In Proceedings of the IEEE International Conference on Robotics and Automation (ICRA), Shanghai, China, 9–13 May 2011; pp. 1–4, doi:10.1109/ICRA.2011.5980567.

28. Samaan, M.; Héno, R.; Pierrot-Deseilligny, M. Close-range photogrammetric tools for small 3d archaeological objects. *Int. Arch. Photogramm. Remote Sens. Spat. Inf. Sci.* **2013**, *15-5(W2)*, 549–553.

29. Sambuelli, L.; Böhm, G.; Capizzi, P.; Cardarelli, E.; Cosentino, P. Comparison between GPR measurements and ultrasonic tomography with different inversion algorithms: An application to the base of an ancient Egyptian sculpture. *J. Geophys. Eng.* **2011**, *8*, 106–116, doi:10.1088/1742-2132/8/3/S10.

30. Sambuelli, L.; Böhm, G.; Colombero, C.; Filipello, A. Photogrammetry and 3-D Ultrasonic Tomography to Estimate the Integrity of Two Sculptures of the Egyptian Museum of Turin. In Proceedings of the Near Surface Geoscience 2015—21st European Meeting of Environmental and Engineering Geophysics, Non-destructive Tests and Prospections for Cultural Heritage, Turin, Italy, 6–10 September 2015; doi:10.3997/2214-4609.201413675.

31. Santos, P.; Ritz, M.; Tausch, R.; Schmedt, H.; Monroy, R.; De Stefano, A.; Posniak, O.; Fuhrmann, C.; Fellner, D.W. CultLab3D: On the Verge of 3D Mass Digitization. In Proceedings of the GCH 2014—Eurographics Workshop on Graphics and Cultural Heritage, Darmstadt, Germany, 6–8 October 2014; pp. 65–73, doi:10.2312/gch.20141305.

32. Scopigno, R.; Callieri, M.; Dellepiane, M.; Ponchio, F.; Potenziani, M. Delivering and using 3D models on the web: Are we ready? *Virtual Archaeol. Rev.* **2017**, *8*, 1–9, doi:10.4995/var.2017.6405.

33. Trampert, J.; Leveque, J. Simultaneous iterative reconstruction technique: Physical interpretation based on the generalized least square solution. *J. Geophys. Res.* **1990**, *95*, 12553–12559, doi:10.1029/JB095iB08p12553.

34. Verstockt, S.; Gerke, M.; Kerle, N. Geolocalization of Crowdsourced Images for 3-D Modeling of City Points of Interest. *IEEE Geosci. Remote Sens. Lett.* **2015**, *12*, 1670–1674, doi:10.1109/LGRS.2015.2418816.

35. Wielandt, E. On the validity of the ray approximation for interpreting delay times. In *Seismic Tomography*; Springer: Dordrecht, The Netherlands, 1987; pp. 85–98, doi:10.1007/978-94-009-3899-1_4.